

ASTROPHYSICAL NEUTRON CAPTURE RATES IN s- AND r-PROCESS NUCLEOSYNTHESIS

H. Beer

*Forschungszentrum Karlsruhe, Institut für Kernphysik III,
P.O. Box 3640, D-760216 Karlsruhe, Germany*

P. Mohr, H. Oberhummer

*Institut für Kernphysik, TU Wien,
Wiedner Hauptstraße 8-10, A-1040 Vienna, Austria*

T. Rauscher

*Institut für Physik, Universität Basel,
Klingelbergstraße 82, CH-4056 Basel, Switzerland*

P. Mutti, F. Corvi

*CEC, JRC, Institute for Reference Materials and Measurements,
Retieseweg, B-2440 Geel, Belgium*

P. V. Sedyshev, Yu. P. Popov

*Frank Laboratory of Neutron Physics, JINR,
141980 Dubna, Moscow Region, Russia*

Abstract: Astrophysical neutron capture rates of light and heavy nuclei have been measured and calculated. For the measurements the activation technique was applied at the 3.75 MV Karlsruhe Van de Graaff accelerator, and at the Geel electron linear accelerator (GELINA) the time-of-flight (TOF) method was used. The calculations were performed using direct and compound nuclear capture models.

1. Introduction

The formation of the chemical elements in the astrophysical s- and r-process scenarios is controlled by astrophysical neutron capture rates at thermonuclear energies in the range at 5 to 250 keV. At these low projectile energies the reaction energy in the capture process mainly comes from the neutron binding energy. As, in general, heavy nuclei have a high density of excited states at this energy the well-known compound nuclear capture reaction mechanism (CN) is dominant. But in light, especially, neutron-rich isotopes, and in isotopes at or close to magic neutron and/or proton shells only few excited states are expected. In these cases besides the compound capture another another capture mechanism, direct capture (DC), is comparable or even dominant.¹⁻¹⁰ In the measurements activation techniques and the time-of-flight method were employed. The measurements were analyzed and the results compared with compound and direct capture model calculations. Cross sections of unstable target nuclei were estimated theoretically. The astrophysical capture rates were applied in s-process calculations.

2. Activation Measurements

2.1. Activation Method

In the activation method a sample of the target isotope is irradiated by a neutron spectrum of a well-defined energy distribution, and the cross section is determined from the activity

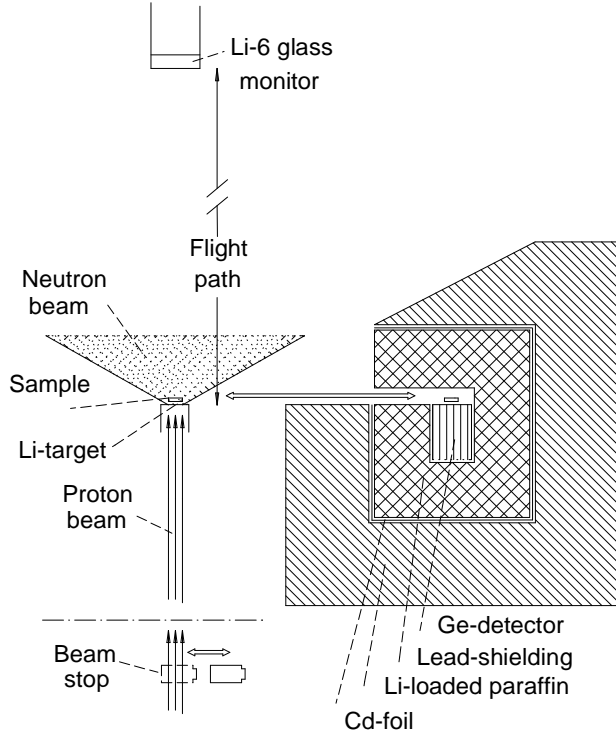


Figure 1: Setup of the fast cyclic activation technique.

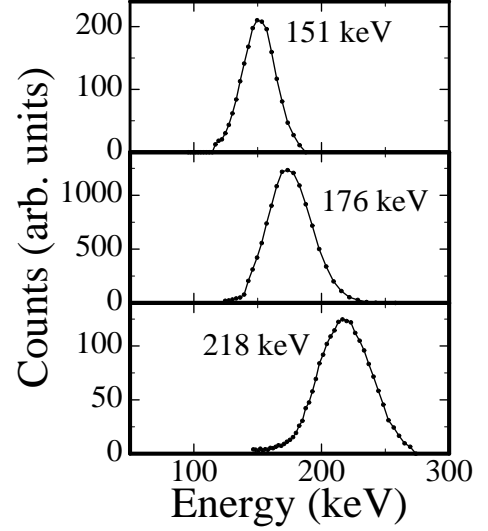


Figure 2: Neutron spectra used for activation.

of the residual nuclei. Because of the short half-lives of many product isotopes a special activation method^{11,12} had to be developed at the Karlsruhe 3.75 MV Van de Graaff accelerator, the cyclic activation technique, where the irradiation and activity counting phases which form an activation cycle are repeated many times (Fig. 1). In the cyclic activation method the time constants for each cycle adjusted to the decay rate λ of the investigated isotope are the irradiation time t_b , the counting time t_c , the waiting time t_w (the time to switch from the irradiation to the counting phase), and the total time $T = t_b + t_w + t_c + t'_w$ (t'_w the time to switch from the counting to the irradiation phase). The accumulated number of counts from a total of n cycles, $C = \sum_{i=1}^n C_i$, with the C_i , the counts of the i -th cycle, irradiated by a neutron flux Φ_i , is given by

$$C = \epsilon_\gamma K_\gamma f_\gamma \lambda^{-1} [1 - \exp(-\lambda t_c)] \exp(-\lambda t_w) \frac{1 - \exp(-\lambda t_b)}{1 - \exp(-\lambda T)} N \sigma [1 - f'_b \exp(-\lambda T)] \sum_{i=1}^n \Phi_i \quad (1)$$

$$\text{with} \quad f'_b = \sum_{i=1}^n \Phi_i \exp[-(n-i)\lambda T] / \sum_{i=1}^n \Phi_i dt \quad .$$

The following quantities have been defined: ϵ_γ : Ge-efficiency, K_γ : γ -ray absorption, f_γ : γ -ray intensity per decay, N : the number of target nuclei, σ : the capture cross section. The activities of nuclides with half-lives of several hours to days can also be counted after the end of the cyclic activation consisting of n cycles:

$$C_n = \epsilon_\gamma K_\gamma f_\gamma \lambda^{-1} [1 - \exp(-\lambda T_M)] \exp(-\lambda T_W) [1 - \exp(-\lambda t_b)] N \sigma f'_b \sum_{i=1}^n \Phi_i \quad (2)$$

Here T_M is the measuring time of the Ge-detector and T_W the time elapsed between the end of cyclic activation and beginning of the new data acquisition. To avoid the absolute

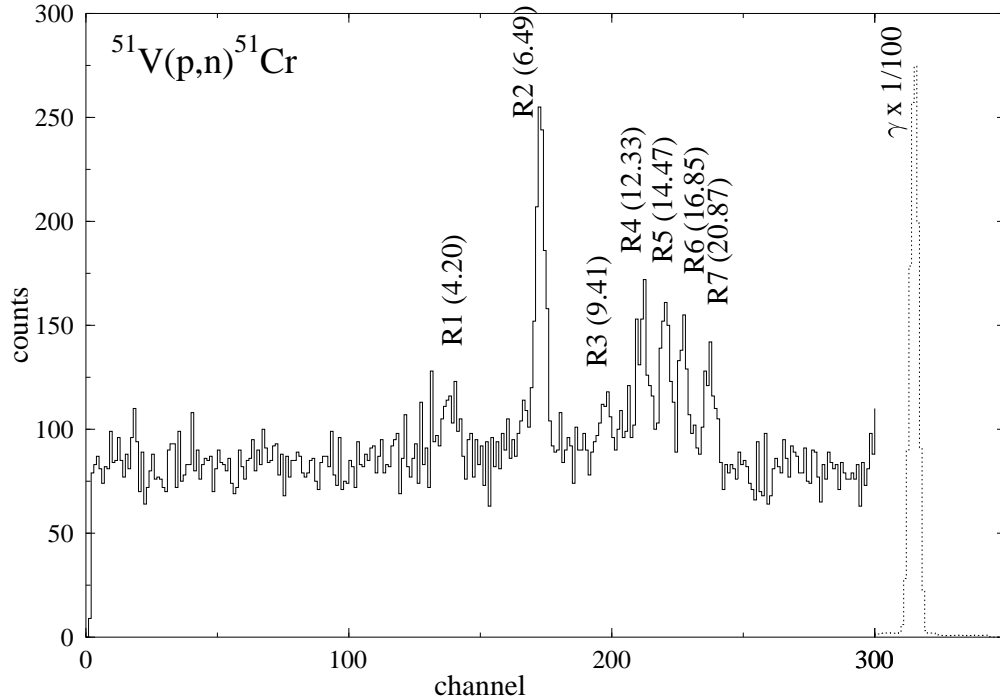


Figure 3: TOF-spectrum of the neutrons from the $^{51}\text{V}(\text{p},\text{n})^{51}\text{Cr}$ reaction close to the reaction threshold.

measurement of the neutron flux the sample to be investigated is sandwiched between two thin gold foils and the capture cross section σ is determined relative to the well-known ^{197}Au cross section.¹³

Normally the neutrons are generated by the $^7\text{Li}(\text{p},\text{n})$ and $\text{T}(\text{p},\text{n})$ reactions. For the energy points at 25 keV and 52 keV one can take advantage of the special properties of these reactions at the reaction threshold. For neutron energies above 100 keV the $^7\text{Li}(\text{p},\text{n})$ reaction is applied at higher proton energies and with thin Li-targets (full half-width 15–20 keV). Examples of generated neutron spectra used in the measurements are shown in Fig. 2. For light isotopes reactor neutrons at 25.3 meV can be an important supplement of the measurements. This has been demonstrated for ^{36}S ⁴ and above all for ^{48}Ca .^{5,9} Additionally, it is desirable to use neutrons in the energy range 5 to 12 keV. In our investigations of (p,n) reactions of different isotopes at reaction threshold we found two possible candidates. With the $^{51}\text{V}(\text{p},\text{n})$ reaction neutrons around 6 keV can be generated. The Fig. 3 shows a time-of-flight spectrum of the $^{51}\text{V}(\text{p},\text{n})$ reaction with a prominent resonance at 6.49 keV. A similar neutron source for neutrons of 8 keV represents the $^{45}\text{Sc}(\text{p},\text{n})$ reaction. This reaction is still under investigation.

2.2. ^{26}Mg and ^{48}Ca Measurements

Astrophysical neutron capture rates of light isotopes are required for inhomogeneous big bang scenarios, the α -rich freeze out, and the s-process of light isotopes to study neutron poisons, the s-process production of rare neutron-rich isotopes (^{36}S , ^{40}Ar), and isotopic anomalies (Si, Ti)¹⁴. Neutron capture of light isotopes at the border of β stability is often dominated by the direct capture mechanism due to the lack of resonance states of the compound system. Direct capture is a smoothly varying cross section normally smaller than 1 mbarn in the energy range above 1 keV. In the Figs. 4,6 the recent results of the measurements on ^{26}Mg ⁸ and ^{48}Ca ⁹ are shown. The data can be described adequately theoretically by the direct capture process.^{1,15} In the keV energy range ^{26}Mg lies in a

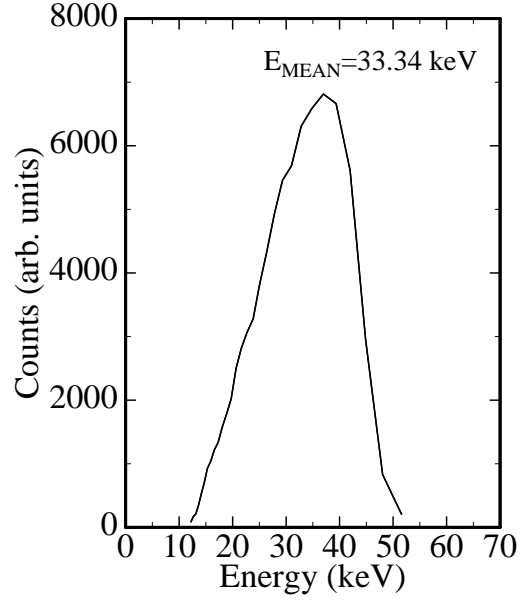
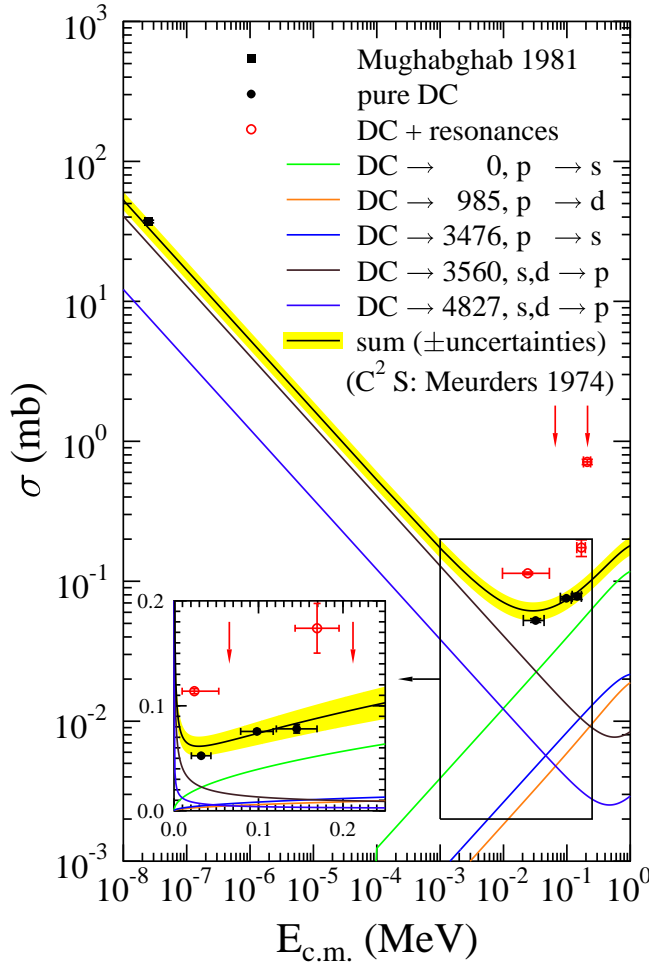


Figure 4: Comparison of the DC cross section for $^{26}\text{Mg}(n,\gamma)^{27}\text{Mg}$ with the experimental data from thermal old of the $^{7}\text{Li}(p,n)$ reaction used for the measurement to thermonuclear projectile energies. The DC contributions for different transitions to the final states of ^{27}Mg as well as the sum of all transitions (solid curve) are shown.

Figure 5: Neutron spectrum at the threshold of the $^{7}\text{Li}(p,n)$ reaction used for the measurement of the ^{26}Mg cross section at 33 keV. Note that with these neutrons the resonance at 68.7 keV is not excited.

transition region from s- to p-wave direct capture. Therefore, the cross section (Fig. 4) which is decreasing up to 30 keV is increasing towards higher energies.⁸ The total DC capture is the sum of many individual transitions. This would make its measurement via these individual partial transitions complicated. At three of the six data points the DC capture is superimposed by compound capture of individual resonances at 68.7 and 220 keV (arrows in Fig. 4). The influence of the 68.7 keV resonance on our value at 33 keV was excluded by choosing a neutron spectrum at the threshold of the $^{7}\text{Li}(p,n)$ reaction (Fig. 5). In Fig. 6 our^{5,9} and previous¹⁶ ^{48}Ca measurements at thermonuclear energies are summarized. Our new data point at 52 keV confirms the $1/v$ behavior of this cross section which is the result of direct s-wave capture. No sign of a destructive interference between the non-resonant direct capture and a hypothetical $1/2^+$ s-wave resonance at 1.5 keV was found.⁵

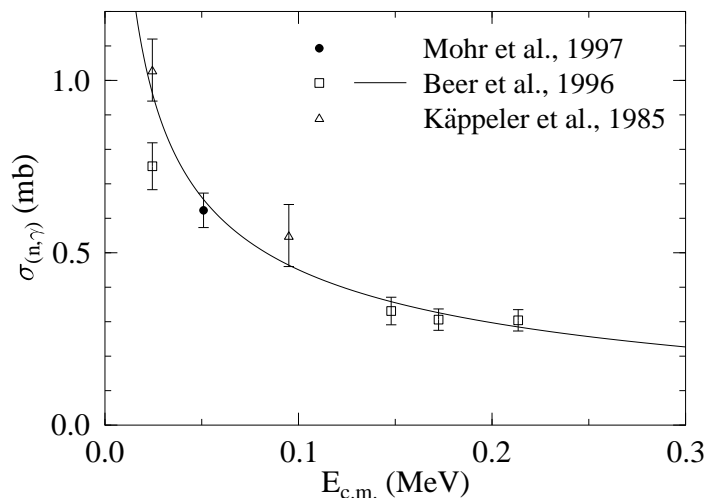


Figure 6: Comparison of the DC cross section for $^{48}\text{Ca}(n,\gamma)^{49}\text{Ca}$ with the experimental data at thermonuclear projectile energies.

2.3. Measurements of Pt-Isotopes

The Pt-isotopes have not yet been investigated by a time-of-flight experiment. With the activation technique capture measurements of $^{190,194,196,198}\text{Pt}$ could be performed with natural Pt samples (metallic foils of 6 mm diameter) even for the rare ^{190}Pt isotope (isotopic content 0.01 %). Although the half lives of the generated activities reach from 13.6s to 4d all isotopic cross sections could be measured in one run. The Figs. 7,8 show the γ -ray activities of the individual Pt-isotopes accumulated during and after termination of the cyclic activation measurement. During the cyclic activation γ -line intensities of all isotopes also of those with short lived activities can be observed (Fig. 7), whereas after the cyclic activation only the long lived activities are accumulated (Fig. 8). This demonstrates that the cyclic activation technique is an extension of the common activation method¹¹ and, therefore, applicable to radioactivities of short and long half-lives as well.¹² It is free of saturation effects which limit the reasonable irradiation time of a common activation. The results of our measurements¹⁷ are shown in Fig. 9 together with estimates for the isotopes $^{192,195}\text{Pt}$. Additionally statistical model calculations with the code SMOKER¹⁸ have been carried out. In Fig. 9 also a comparison is made between our measured and theoretically calculated Pt Maxwellian average capture (MAC) cross sections (BR)¹⁷ and previous theoretical results from (AGM)¹⁹, (HWFZ)²⁰, (Harris)²¹, and (CTT)²². Excellent agreement between experimental and theoretical values was found for our MAC cross sections.

The s-process nucleosynthesis path in the Os to Pt mass region is shown in Fig. 10. For ^{191}Os , ^{192}Ir , and ^{193}Pt there is a competition between β -decay and neutron capture. The β -decay half lives are dependent on temperature and electron density of the s-process environment.²³ The abundance of s-only ^{192}Pt originates from the branchings at ^{191}Os and ^{192}Ir . The isotopes ^{190}Pt and ^{198}Pt are not on the s-process path, therefore the seed abundances vanish during nucleosynthesis. Calculations to reproduce the s-process abundances in the Os- to Pt-mass region have been carried out using parametrized models described in detail elsewhere.¹⁰ In the analysis of the present branching especially the neutron density was adjusted to reproduce the solar abundance of the s-only isotope ^{192}Pt . The calculations were carried out taking into account the uncertainties of the

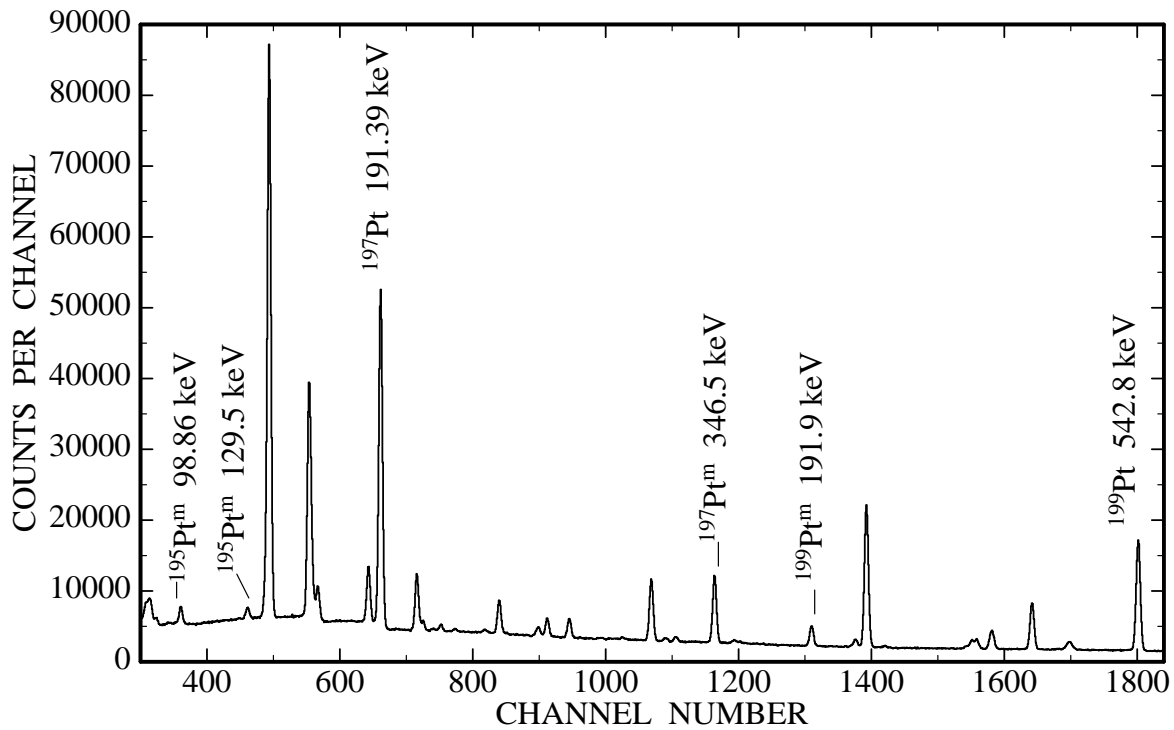


Figure 7: Accumulated intensities of decay γ -ray lines from ^{195m}Pt , ^{197}Pt , ^{197m}Pt , ^{199}Pt , and ^{199m}Pt . Accumulation of 4224 activation cycles.

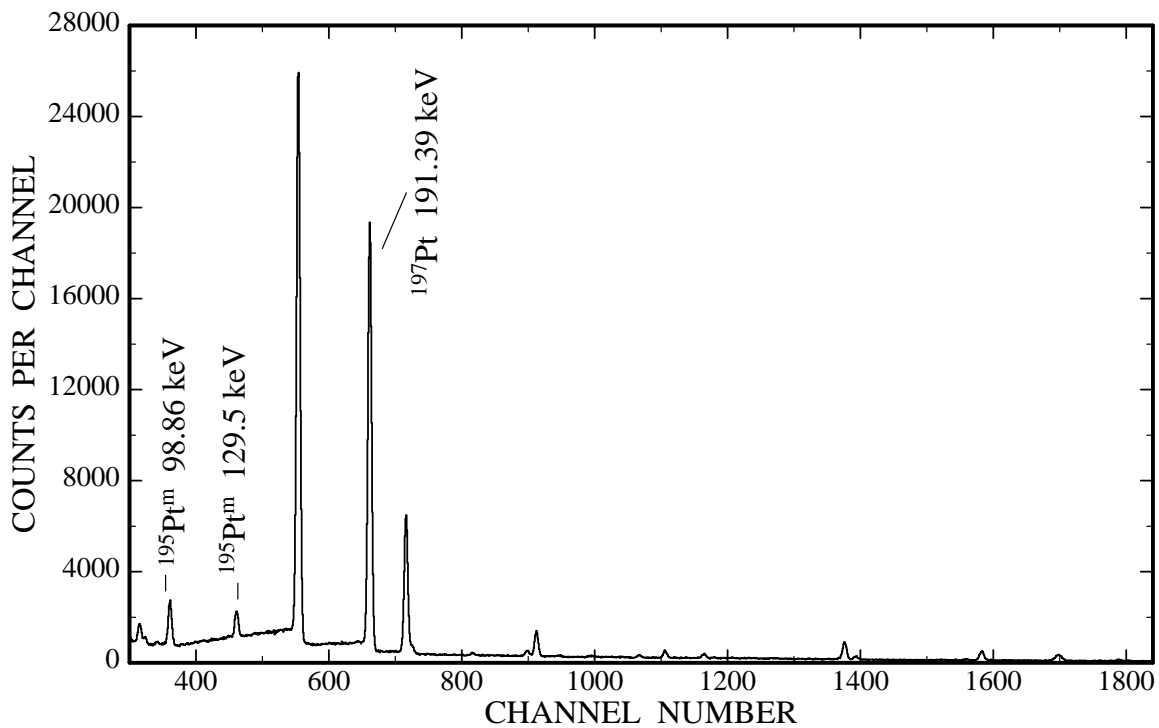


Figure 8: The intensities of decay γ -ray lines from ^{195m}Pt and ^{197}Pt . The data acquisition after the termination of the cyclic activation run. Note that in this case only the long lived activities can be counted.

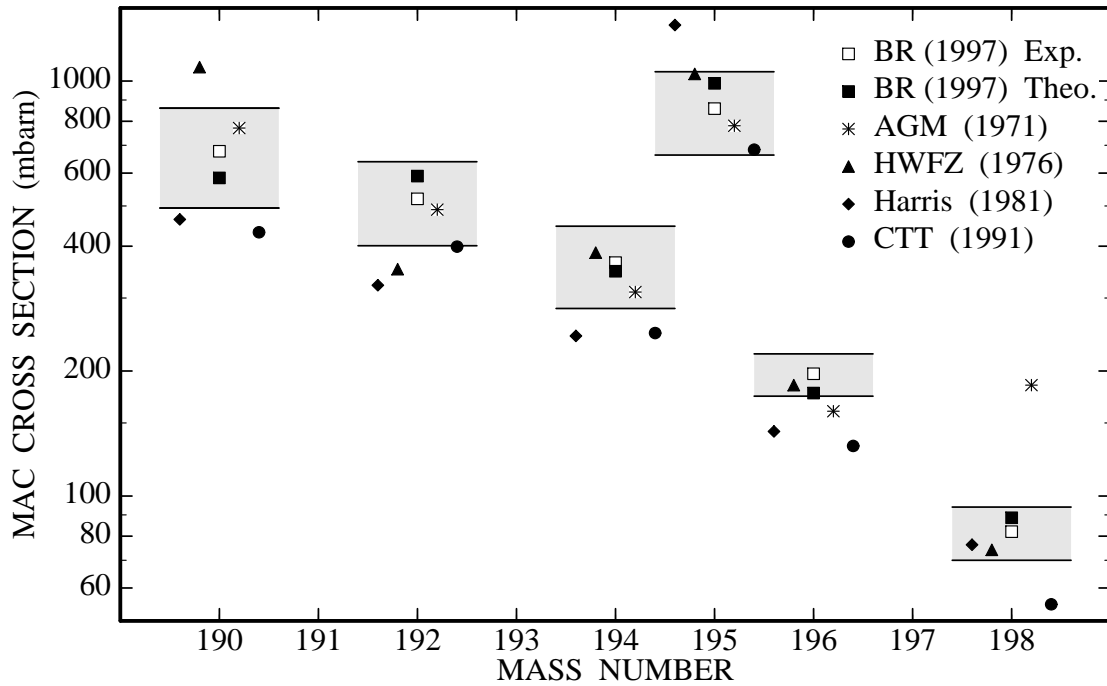


Figure 9: MAC cross sections of the stable Pt-isotopes at $kT=30$ keV. Comparison of the experimentally and theoretically determined values of Beer and Rauscher (BR 1997) with theoretical estimates from literature. Note that the theoretically calculated values of BR (1997) agree with the experimental estimates within quoted uncertainties (shaded area). The references of the different abbreviations in the figure are given in the text.

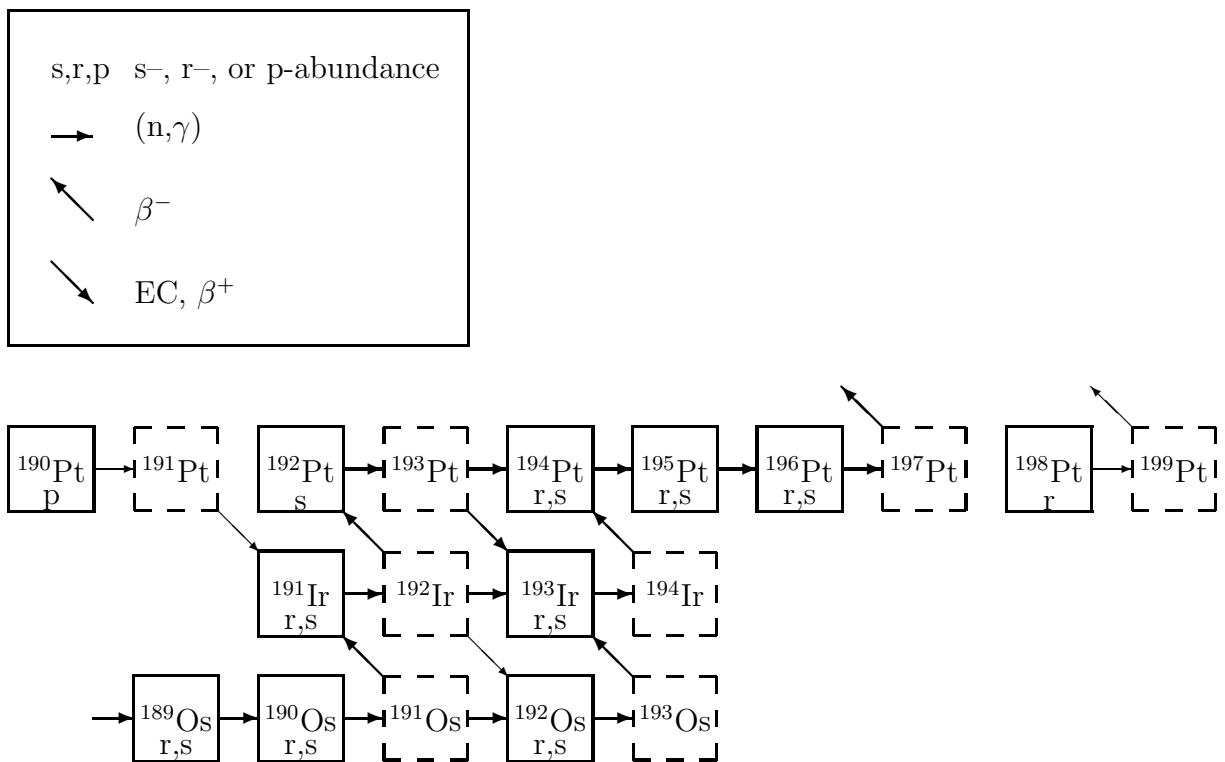


Figure 10: s-process path between Os and Pt. The solid boxes are the stable isotopes. The origin of nucleosynthesis is indicated. If there are two contributions, the major contribution is designated first. The dashed boxes are radioactive nuclei.

MAC cross sections and the solar ^{192}Pt abundance. At the neutron density $5.0 \times 10^8 \text{ cm}^{-3}$ which was deduced using all s-process branchings¹⁰ the ^{192}Pt abundance appears to be distinctly underproduced compared with the respective solar abundance. Only at definitely lower neutron densities ($\leq 3.2 \times 10^8 \text{ cm}^{-3}$) the calculated abundance values become consistent with the range of empirical ^{192}Pt values. This distinct difference between neutron densities describing all s-process branchings on the average and the smaller values found for the ^{191}Os - and ^{192}Ir -branchings could be the effect of freeze-out for the $^{22}\text{Ne}(\alpha, n)$ neutron source. To confirm this effect the MAC cross sections of the unstable ^{191}Os and ^{192}Ir isotopes have to be determined to better than 20 %.

3. Time-of-Flight Measurements

3.1. ^{136}Ba and ^{209}Bi Results

Among the heavy nuclei the isotopes near or at magic neutron shells have got the smallest capture cross sections. These bottleneck isotopes which control the s-process nucleosynthesis are characterized below 100 keV neutron energy by resonance structure which can be well resolved in high resolution time-of-flight measurements. At the electron linear accelerator GELINA in Geel, Belgium, neutron capture measurements of the bottleneck isotopes ^{138}Ba and ^{208}Pb have been carried out using a pair of C_6D_6 liquid scintillation detectors at the 60 m flight path station.¹⁰ Details of the detection geometry and the characteristics of the detector efficiency can be found elsewhere.²⁴ These experiments were continued with new measurements of ^{136}Ba ²⁵ and ^{209}Bi ²⁶. Both measurements are in agreement within quoted uncertainties with previous results.^{27,28,29} The stellar rate of s-only ^{136}Ba is now one of the best known astrophysical rates.^{25,27,28} It should be noted that the MAC cross section of ^{209}Bi at $kT=30 \text{ keV}$ reported by Mughabghab²⁹ is an erroneous calculation from the resonance parameters.

With these reliable MAC cross sections of the bottleneck isotopes the s-process calculations were improved. Parametrized s-process model calculations have been carried out.¹⁰ In the standard SP-model it is attempted to fit global and local structures of the synthesis by one major neutron source burning at $kT=27.1 \text{ keV}$. A better reproduction of the solar s-process abundances was obtained in the DP-model by combined burning of two neutron sources ignited at $kT=8$ and 28 keV , respectively. The new MAC cross section of ^{209}Bi confirms this s-process analysis at the termination of the synthesis.¹⁰ The special role of the ^{138}Ba MAC cross section and the new measurement of ^{136}Ba ²⁵ also allows a more detailed investigation of the isotopic anomalies in barium ascribed to the s-

Table 1: Ba isotopic ratios. A non-solar s-process composition can be assumed for s-Ba from meteoritic SiC grains. In brackets the results expected from a solar s-process composition.

	τ_0 (mbarn ⁻¹)	134/136	135/136	137/136	138/136
solar ratios ^a		0.308	0.839	1.430	9.129
s-Ba ^b		0.341±0.003	0.135±0.003	0.684±0.007	6.22±0.08
SP model	0.188 (0.296)	0.37 (0.35)	0.15 (0.14)	0.74 (0.75)	6.22 (7.89)
DP model	0.102 (0.140)	0.31 (0.30)	0.16 (0.15)	0.76 (0.76)	6.22 (7.21)

^a Ref.³⁰, ^b Ref.³¹

process. In Table 1 Ba isotopic ratios obtained from s–process calculations are compared with the observed s–Ba ratios detected in meteoritic SiC grains³¹. Additionally the solar ratios are given, too. The isotopic chain of Ba has got unique s–process features. The abundance ratio of the s–only isotopes $^{134}\text{Ba}/^{136}\text{Ba}$ depends on a branching at ^{134}Cs which is sensitive to both s–process neutron density and temperature. The isotope ^{138}Ba controls the average neutron exposure τ_0 in the s–process. The character of this dependence shows the ratio

$$^{138}\text{Ba}/^{137}\text{Ba} = (\sigma_{138} + \tau_0^{-1})^{-1}/(\sigma_{137})^{-1} \quad , \quad (3)$$

where the MAC cross section σ_{138} is comparable with τ_0^{-1} . A necessary condition that the exposure sensitivity of the successive Ba–isotopes 136, 137, and 138 on the unique synthesis path can be studied is the fact that $^{138}\text{Ba}/^{136}\text{Ba}$ is significantly less than $(\sigma_{138})^{-1}/(\sigma_{136})^{-1}$, i.e., there is a strong deviation from the anticorrelation between abundance and MAC cross section (compare e.g., the s–process $^{138}\text{Ba}/^{136}\text{Ba}$ ratios of Tab. 1 with $(\sigma_{138})^{-1}/(\sigma_{136})^{-1} = 13.26$ at $kT=8\text{keV}$). In the SP– and DP–model calculations the exposure τ_0 has been adjusted to reproduce the $^{138}\text{Ba}/^{136}\text{Ba}$ ratio. The s–Ba composition seems to be different from the solar s–process (in brackets in Tab. 1) because the ratio $^{138}\text{Ba}/^{136}\text{Ba}$ is different and consequently also the average exposure (Table 1).

The support of the Volkswagen–Stiftung (Az: I/72286), the Deutsche Forschungsgemeinschaft (DFG) (project Mo739) and the Fonds zur Förderung der wissenschaftlichen Forschung (FWF S7307–AST) is gratefully acknowledged. TR is supported by an APART fellowship of the Austrian Academy of Sciences.

References

1. H. Oberhummer, H. Herndl, T. Rauscher, and H. Beer, *Surveys in Geophys.*, **17** (1996) 665
2. H. Beer, G. Rupp, F. Voß, and F. Käppeler, *Ap. J.* **379** (1991) 420
3. H. Beer, M. Wiescher, F. Käppeler, J. Görres, and P. E. Koehler, *Ap. J.* **387** (1992) 258
4. H. Beer, P. V. Sedyshev, Yu. P. Popov, W. Balogh, H. Herndl, and H. Oberhummer, *Phys. Rev.* **C52** (1995) 3442
5. H. Beer, C. Coceva, P. V. Sedyshev, Yu. P. Popov, H. Herndl, R. Hofinger, P. Mohr, and H. Oberhummer, *Phys. Rev.* **C54** (1996) 2014
6. J. Meißner, H. Schatz, J. Görres, H. Herndl, M. Wiescher, H. Beer, and F. Käppeler, *Phys. Rev.* **C53** (1996) 459
7. J. Meißner, H. Schatz, H. Herndl, M. Wiescher, H. Beer, and F. Käppeler, *Phys. Rev.* **C53** (1996) 977
8. P. Mohr, H. Oberhummer, and H. Beer, *Proc. of the Int. Symposium on Capture Gamma–Ray Spectroscopy and Related Topics*, ed. G. Molnar, Budapest 1996, in print
9. P. Mohr, H. Oberhummer, H. Beer, W. Rochow, V. Knölle, G. Staudt, P. V. Sedyshev, and Yu. P. Popov, *Phys. Rev.* **C**, submitted
10. H. Beer, F. Corvi, and P. Mutti, *Ap. J.* **474** (1997) 843
11. H. Beer and F. Käppeler, *Phys. Rev.* **C21** (1980) 534
12. H. Beer, G. Rupp, G. Walter, F. Voß, and F. Käppeler, *Nucl. Instr. Methods* **A337** (1994) 492
13. W. Ratynski and F. Käppeler, *Phys. Rev.* **C37** (1988) 595; and R. L. Macklin, private communication

14. P. Hoppe, S. Amari, E. Zinner, T. Ireland, and R. S. Lewis, *Ap. J.* **430** (1994) 870
15. K. H. Kim, M. H. Park, and B. T. Kim, *Phys. Rev.* **C35** (1987) 363
16. F. Käppeler, G. Walter, and G. J. Mathews, *Ap. J.* **291** (1985) 319
17. H. Beer and T. Rauscher, *Ap. J.*, submitted
18. F.-K. Thielemann, M. Arnould, and J. W. Truran, in *Adv. in Nucl. Astrophys.*, eds. E. Vangioni-Flam et al. (Gif-sur-Yvette: Editions Frontières 1987), p. 525
19. B. J. Allen, J. H. Gibbons, and R. L. Macklin, *Adv. Nucl. Phys.*, **375** (1971) 823
20. J. A. Holmes, S. E., Woosley, W. A. Fowler, and B. A. Zimmerman, *At. Data Nucl. Data Tables* **18** (1976) 306
21. M. J. Harris 1981, *Astrophys. Space Sci.* **77** (1981) 357
22. J. J. Cowan, F.-K. Thielemann, and J. W. Truran, *Phys. Rep.*, **208** (1991) 267
23. K. Takahashi and K. Yokoi, *Atomic Data Nucl. Data Tables* **36** (1987) 375
24. F. Corvi, G. Fioni, F. Gasperini, and P. B. Smith, *Nucl. Sci. Eng.* **107** (1991) 272
25. P. Mutti, F. Corvi, K. Athanassopulos, and H. Beer, in *Nuclei in the Cosmos*, Notre Dame, USA, 20.–27. June, 1996, ed. M. Wiescher, *Nucl. Phys. A (Suppl.)*, in print
26. P. Mutti, F. Corvi, K. Athanassopulos, and H. Beer, *Int. Conf. on Nuclear Data for Science and Technology*, Trieste, Italy, 19.–24. May, 1997
27. F. Voss, K. Wisshak, and F. Käppeler, *Phys. Rev.* **C52** (1995) 1102
28. P. E. Koehler, R. R. Spencer, R. R. Winters, K. H. Guber, J. A. Harvey, N. W. Hill, and M. S. Smith, *Phys. Rev.* **C54** (1996) 1463
29. S. F. Mughabghab, *Neutron Cross Sections, Vol 1, Part B* (Academic Press, INC., Orlando 1984)
30. H. Palme and H. Beer, in *Landolt Börnstein, New Series VI, Astronomy and Astrophysics, Subvolume 3a*, (Berlin: Springer 1993), p. 196
31. C.A. Prombo, F.A. Podosek, S. Amari, and R.S. Lewis, *Ap. J.* **410** (1990) 393